



Present-day in situ stress prediction in Bozi 3 deep sandstone reservoir, Kuqa Depression: implications for gas development

Hui Zhang¹ · Wei Ju² · Ke Xu¹ · Peiming Huang² · Yu Zhong² · Xinyu Liu¹ · Xinxin Wang¹ · Zhimin Wang¹ · Shujun Lai¹

Received: 15 April 2021 / Accepted: 3 July 2021 / Published online: 20 July 2021
© Saudi Society for Geosciences 2021

Abstract

Resources, including petroleum and natural gas, from deep and ultra-deep reservoirs have become an important contributor to global reserve growth and deliverability construction. Knowledge of the present-day in situ stress field has significant applications for efficient exploration and development. The Bozi 3 deep sandstone reservoir is important for increasing natural gas production in the Kuqa Depression. However, little attention has been given to the present-day in situ stress state of the Bozi 3 Block. In this study, the in situ stress orientation and magnitudes were investigated based on stress indicator interpretation, well log calculation, and geomechanical modeling. Drilling-induced tensile fractures and borehole breakouts indicated a dominant NW-SE direction for the horizontal maximum principal stress (S_{Hmax}) in the Bozi 3 deep sandstone reservoir. The stress regime for the Bozi 3 Block indicates a dominant strike-slip faulting type ($S_{Hmax} \geq S_v \geq S_{Hmin}$). Numerical simulation of the present-day in situ stresses showed that the S_{Hmax} and horizontal minimum principal stress (S_{Hmin}) magnitudes were $-150 \sim -178$ MPa and $-121 \sim -157$ MPa in the Cretaceous, respectively. Natural fractures are generally stable in the present-day stress field. When the specific gravity reaches 2.15, approximately 75% of all natural fractures are reactivated. Under the present-day stress state in the Bozi 3 Block, new horizontal wells should be drilled with ENE-WSW-trending. The results for the present-day in situ stress state are expected to provide geological and engineering references for deep gas production in the Bozi 3 Block of Kuqa Depression.

Keywords Present-day in situ stress · Numerical simulation · Well log calculation · Bozi 3 deep sandstone reservoir · Kuqa Depression

Introduction

With increasing depletion of conventional natural resources, more attention has been focused on deep and ultra-deep reservoirs, and natural gas from these reservoirs has become an important contributor to global reserve growth and deliverability construction. Currently, the critical depth for deep and ultra-deep reservoirs varies among different countries, and a standard and unified definition has not emerged because of geological differences (Dyman et al. 1998; Zhang et al.

2015; Feng et al. 2016). In western China, a “deep reservoir” is generally considered to correspond to a burial depth larger than 4500 m, and an “ultra-deep reservoir” corresponds to a depth over 6000 m (Wang 2012). Recent exploration indicates that natural gas resources are abundant within deep and ultra-deep reservoirs in western China, especially the Kelasu tectonic zone of Kuqa Depression, Tarim Basin (Tian et al. 2020; Xu et al. 2020; Zeng et al. 2020).

During drilling process and further development of deep and ultra-deep natural gas resources, an accurate understanding of the distribution of present-day in situ stresses is important to effectively prevent borehole collapses, reduce drilling costs, guide hydraulic fracturing, and improve reservoir management (Zoback et al. 2003; Tingay et al. 2009; Kingdon et al. 2016; Rajabi et al. 2016; Ju et al. 2017, 2018a). Common descriptions of the present-day in situ stress state are based on the magnitudes of vertical stress (S_v), horizontal maximum principal stress (S_{Hmax}), horizontal minimum principal stress (S_{Hmin}), and the orientation of S_{Hmax} (Zoback et al. 2003; Rajabi et al. 2016). The present-day in situ stress state in

Responsible Editor: François Roure

✉ Wei Ju
wju@cumt.edu.cn

¹ Institute of Exploration and Development, PetroChina Tarim Oilfield Company, Korla 841000, China

² School of Resources and Geosciences, China University of Mining and Technology, Xuzhou 221116, China

a sedimentary basin may change both laterally and vertically due to the development and distribution of faults, lithological differences, etc. Anderson delineated three types of stress regimes based on their relative stress magnitudes: the normal faulting stress regime ($S_v > S_{Hmax} > S_{hmin}$), strike-slip faulting stress regime ($S_{Hmax} > S_v > S_{hmin}$), and reverse faulting stress regime ($S_{Hmax} > S_{hmin} > S_v$) (Anderson 1951).

The Bozi 3 Block of Kelasu tectonic zone is a typical deep sandstone reservoir in the Kuqa Depression, which is characterized by low permeability, low porosity, and strong heterogeneity. Therefore, natural gas within this block cannot be produced naturally and production intervention is required to obtain commercial quantity of gas (Holditch 2006; Ju and Wang 2018). Hydraulic fracturing is an important production intervention approach that has proven to be effective for commercial gas development. This approach depends partially on the present-day in situ stress (Zoback 2007; Rajabi et al. 2016; Ju et al. 2020); hence, accurate prediction of the present-day stress field is extremely significant for effective gas production in the Bozi 3 Block of Kuqa Depression.

The present-day in situ stress data can be obtained from actual measurements; however, measured data for the Bozi 3 Block are limited and widely spread over a large scale, precluding discernment of the overall characteristics of the stress distribution. Therefore, the objective of this study is to delineate the present-day in situ stress state of the Bozi 3 Block of Kuqa Depression, based on stress indicator interpretation, well log calculation, and numerical simulation, and to analyze the effects of stress distribution on deep resource development. The results are expected to provide geological references for natural gas production in the study area.

Geologic setting

The Kuqa Depression, known as the Kuche Depression, is located along the northern margin of Tarim Basin with an ENE-WSW trend (Fig. 1). Based on tectonic characteristics, the Kuqa Depression is laterally divided into the northern monocline belt, Kelasu-Yiqikelike structural belt, Baicheng and Yangxia sags, and Qiulitage structural belt from north to south (Fig. 1; Allen and Vincent 1999; Zeng et al. 2010; Ju and Wang 2018). Faults and folds are well developed in the Kelasu-Yiqikelike structural belt (Fig. 1). Furthermore, the Kelasu structural belt can be divided into the Keshen segment, Dabei segment, Bozi segment, and Awate segment from east to west, where the Bozi 3 deep sandstone reservoir is located in the Bozi segment (Fig. 1).

The Bozi 3 Block is a diamond-shaped, deeply buried area in the Kuqa Depression (Fig. 2), within which, the main natural gas production layers are the Cretaceous deposits, including the Bashijiqike (K_1bs) Formation and Baxigai (K_1bx) Formation. The formations mainly consist of a series of

sandstone and mudstone (Fig. 3). Reservoir test results for the entire Bozi segment indicate that the Bashijiqike Formation is characterized by low porosity and permeability. The effective porosity mainly ranges from 3.5 to 10.0% with an average of 6.30%. The matrix permeability varies between 0.10 and 0.50 mD (Wei et al. 2020). These results suggest that technologies, such as hydraulic fracturing, are required to obtain high natural gas production from the Bozi 3 deep sandstone reservoir.

Interpretation of the S_{Hmax} orientation

Many methods can be applied to determine the S_{Hmax} orientation. The most commonly used approach in petroleum and natural gas industry is the interpretation of drilling-induced tensile fractures (DITFs) and borehole breakouts from imaging logs (Zoback 2007; Ju et al. 2017). DITFs generally exhibit two patterns: (1) Pattern I, which symmetrically aligned fractures lie parallel or subparallel to the borehole axis on opposite sides of the borehole wall (Fig. 4a); and (2) Pattern II, in which en-echelon fractures lie around the borehole with traces that are 180° apart (Fig. 4b). Borehole breakouts commonly appear in imaging logs as broad, parallel conductive zones separated by approximately 180° (Fig. 4c).

Previous studies have proven that borehole breakouts have a perpendicular orientation to the S_{Hmax} , and DITFs indicate the orientation of S_{Hmax} (Zoback et al. 2003; Rajabi et al. 2016; Ju and Wang 2018).

In this study, DITFs and borehole breakouts were interpreted from imaging logs of Well Z1, Well Z2, and Well Z3 (Fig. 4). Overall, the S_{Hmax} orientation indicated a dominant NNW-SSE direction (Fig. 5). Additionally, the orientation showed minor variations in different geological locations, which may result from the development of small faults, folds, natural fractures, lithological transitions, or differences (Martin and Chandler 1993; Bell 1996; Ju et al. 2018b).

In situ stresses calculated from wells

Method

Generally, the S_v magnitude is the weight of the overburden, which can be calculated by integrating the rock density from the surface to the measured depth (Zoback et al. 2003; Brooke-Barnett et al. 2015; Ju and Wang 2018) using Eq. (1).

$$S_v = \int_0^z \rho(h)g \, dh \quad (1)$$

where g is the gravitational acceleration, m/s^2 ; $\rho(h)$ is the density of the overburden rock as a function of burial depth, kg/m^3 ; h is the burial depth from the surface to a particular

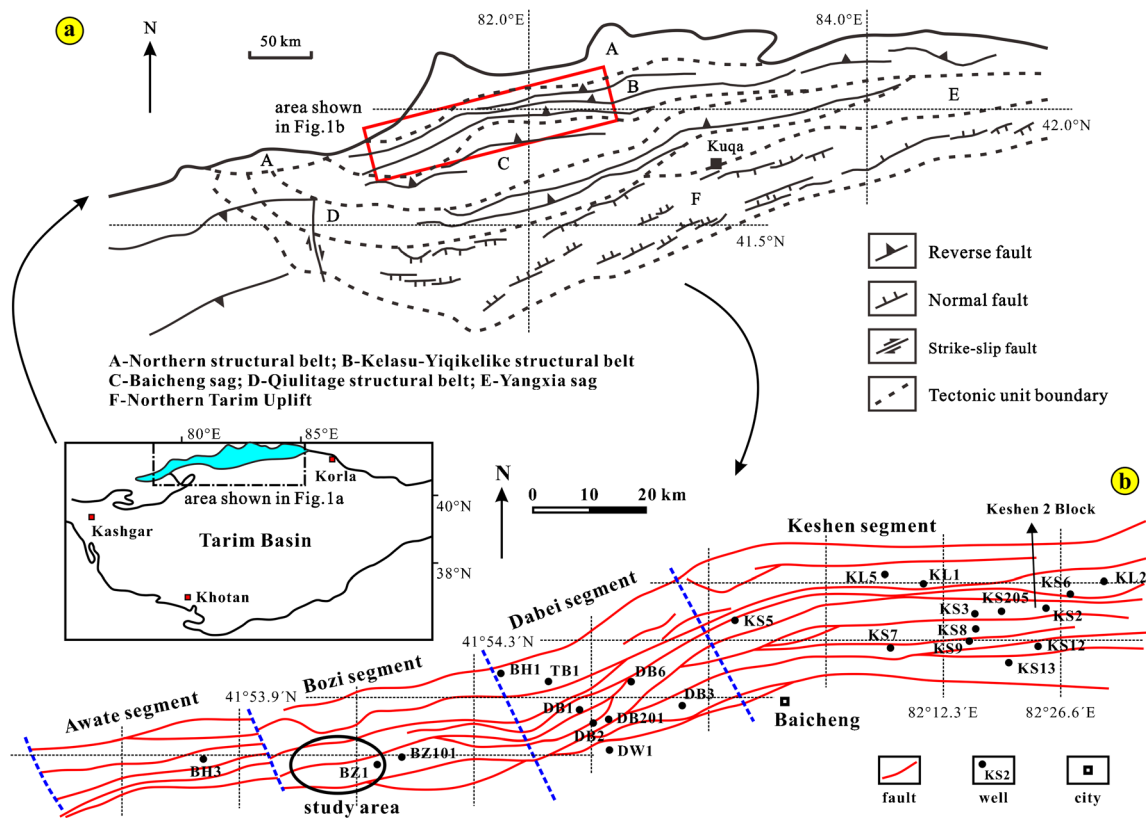


Fig. 1 (a) Structural simplified map of the Kuqa Depression in the Tarim Basin; (b) Structural framework of the Kelasu structural belt

depth underground, m ; z is the target depth, m .

The density logs for the study area are not obtained from the ground level; hence, based on rock mechanics experiments from surface rocks, an extrapolation method with a gradient of approximately 23 kPa/m is used here to determine the S_v magnitude for segments without density logs.

The magnitudes of S_{Hmax} and S_{hmin} in this study are calculated using the revised Anderson model (Eq. 2).

$$\begin{cases} S_{Hmax} = \frac{\mu}{1-\mu}(S_v - \alpha P_0) + \alpha P_0 + S_t \\ S_{hmin} = \frac{\mu}{1-\mu}(S_v - \alpha P_0) + \alpha P_0 + S_t \end{cases} \quad (2)$$

where S_{Hmax} and S_{hmin} are horizontal maximum and minimum principal stress, respectively, MPa; α is the effective stress coefficient (also the Biot coefficient), unitless; μ is the Poisson's ratio, unitless; P_0 is the pore pressure, MPa; S_t

and S_t are the additional tectonic stress corresponding to S_{Hmax} and S_{hmin} , respectively, MPa.

The first term on the right hand of Eq. (2) is a linear elastic term for transforming the vertical stress to horizontal stresses. The second term corresponds to the fluid pressure. The third term is related to external sources of stress, such as the tectonic stress.

In situ stress distribution from log calculations

In this study, the log calculation results for Well Z1 show that the S_{Hmax} and S_{hmin} magnitudes in the Cretaceous deposits range between 126 and 176 MPa, and 99 and 149 MPa, respectively (Fig. 6). The majority of calibrated stress profiles suggest a dominant strike-slip faulting stress regime in the Cretaceous Baxigai Formation (Fig. 6).

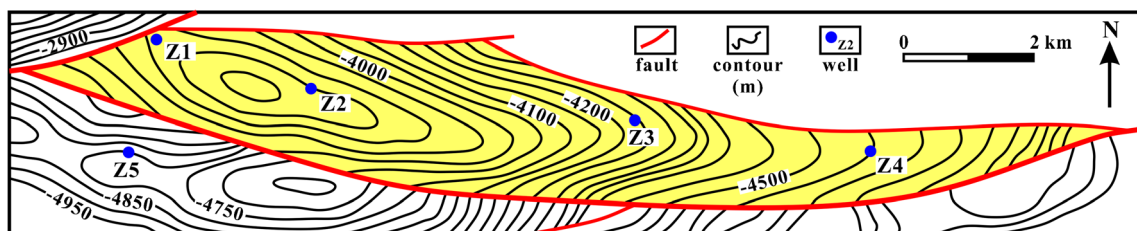


Fig. 2 Structural map of the top Cretaceous in the Bozi 3 Block of Kuqa Depression. The area with yellow background in this figure indicates the Bozi 3 Block

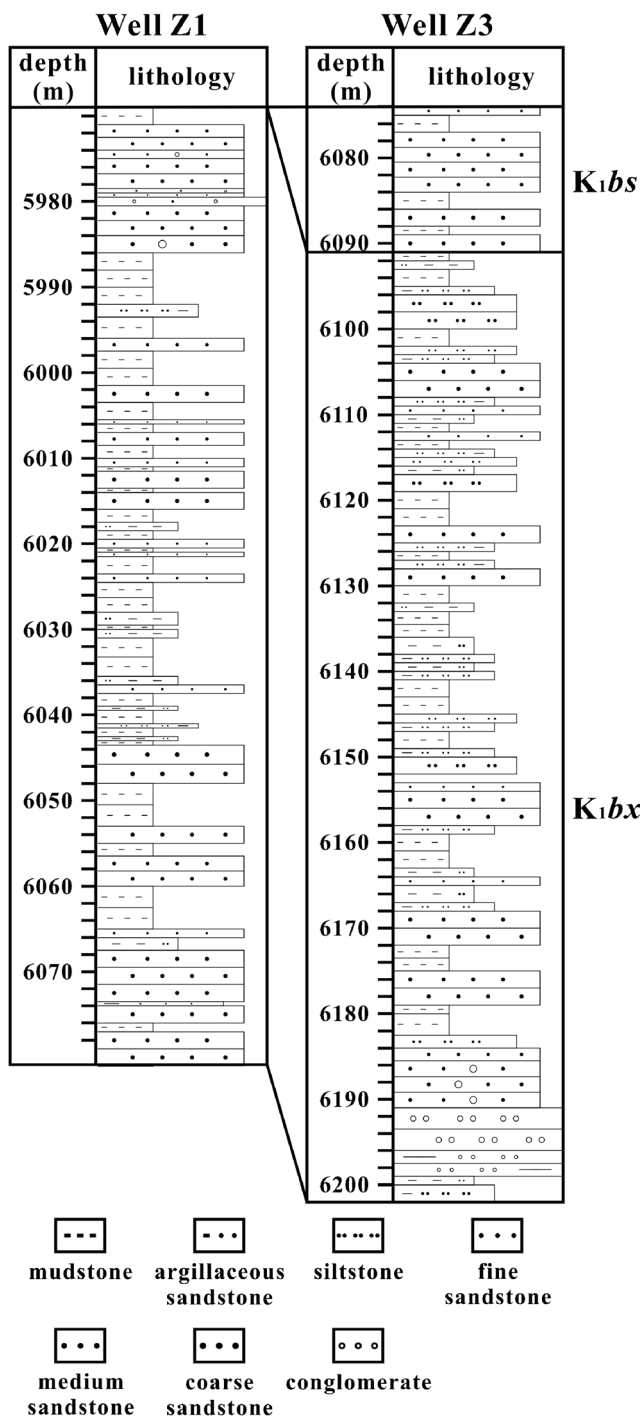


Fig. 3 Stratigraphic column of the Cretaceous in the Bozi 3 Block of Kuqa Depression

Distribution prediction of in situ stresses

Method

A numerical simulation is performed based on the finite element (FE) technique, where a single complete geometric model is firstly built and discretized into a finite number of continuous elements connected by nodes (Ding et al. 2012). Then,

different rock mechanical parameters are assigned to different elements in the geometric model to create a geological model (Ding et al. 2012; Jiu et al. 2013; Ju and Sun 2016). A numerical solution is obtained by transforming the continuous field function of the entire geological body into a node function including basic variations in the stress, strain, and displacement caused by external forces (Ding et al. 2012; Liu et al. 2020).

Elastic mechanics theory is used to express the relationship between the strain and the displacement given in Eq. (3):

$$\begin{cases} \epsilon_{xx} = \frac{\partial i}{\partial x}, & \gamma_{xy} = \gamma_{yx} = \frac{\partial i}{\partial y} + \frac{\partial j}{\partial x} \\ \epsilon_{yy} = \frac{\partial j}{\partial y}, & \gamma_{yz} = \gamma_{zy} = \frac{\partial j}{\partial z} + \frac{\partial k}{\partial y} \\ \epsilon_{zz} = \frac{\partial k}{\partial z}, & \gamma_{zx} = \gamma_{xz} = \frac{\partial k}{\partial x} + \frac{\partial i}{\partial z} \end{cases} \quad (3)$$

where ϵ_{xx} , ϵ_{yy} , and ϵ_{zz} are the linear strain components, and γ_{xy} , γ_{yz} , and γ_{zx} are the shear strain components.

The matrix form is derived as follows (Eq. (4)).

$$[\epsilon] = [B][\delta] \quad (4)$$

where $[\delta]$ is the nodal displacement matrix, $[B]$ is the geometric matrix.

The physical equation can be used to derive the stress and strain given by Eq. (5):

$$[\sigma] = [D][\epsilon] \quad (5)$$

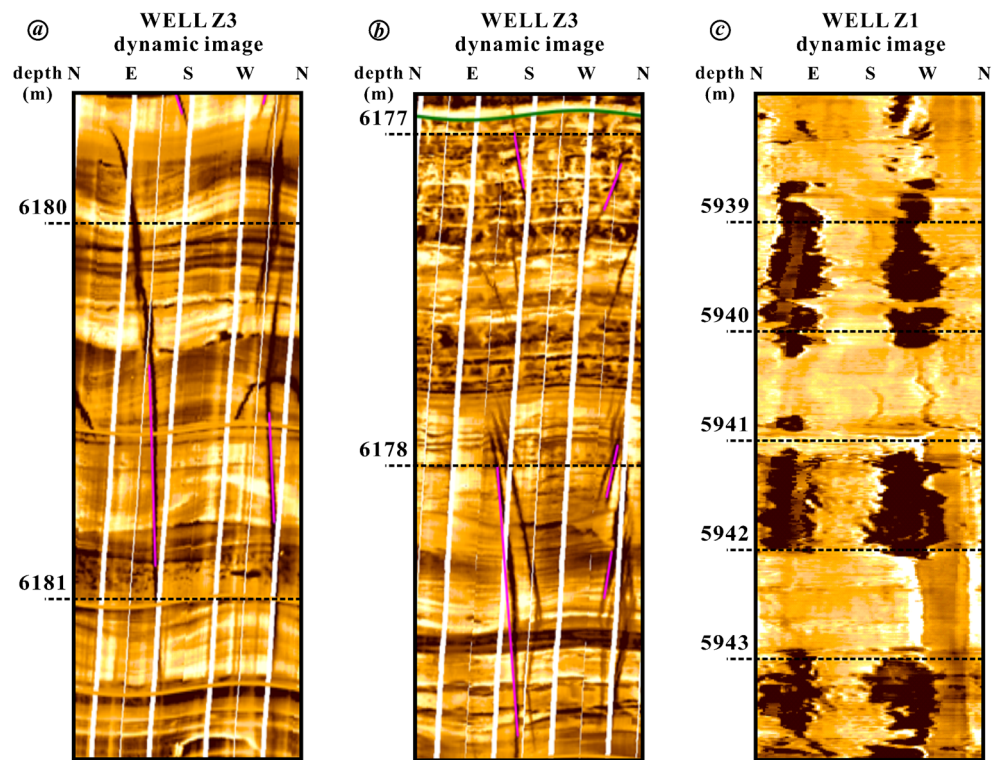
where $[D]$ is the elasticity matrix.

Geological model setup

The geometric model (Fig. 7a) used in this study was established utilizing finite element ANSYS software (version 14.5; Ansys Inc., Houston, USA) following a forward (dot-line-area-volume) setup order based on the basic conditions shown in Fig. 2, which is generally labor-intensive. The building procedure consists of the following steps: (i) choosing an appropriate element type, (ii) generating different solid model features, and (iii) applying Boolean operators or specific number controls to join separate solid model regions together as appropriate.

Then, the mechanical parameters of sedimentary layers were obtained from the results of rock mechanics experiments, and their average values were used in the established geometric model making a geological model (Table 1). Faults inside the model were represented by weakness zones with relatively low Young's moduli (Fischer and Henk 2013; Ju and Sun 2016). The magnitude of Young's moduli are 85% of the corresponding layer based on previous studies (e.g., Jiu et al. 2013; Ju et al. 2018b).

Fig. 4 Drilling-induced tensile fractures and breakouts from borehole imaging logs in the Bozi 3 Block of Kuqa Depression. (a) Well Z3, drilling-induced tensile fractures, pattern I; (b) Well Z3, drilling-induced tensile fractures, pattern II; (c) Well Z1, borehole breakouts



To reduce the calculation complexity and improve the accuracy, all the units in the geological model were discretized using primarily three-node triangular elements (Fig. 7b). Meshing controls were set to obtain the desired mesh density, and nodes and elements were created by meshing the solid model. The entire meshed model contained 80825 nodes and 473069 elements.

Boundary conditions

The study area was nested within a larger rectangular parallelepiped to reduce boundary effects on the modeling results (Fig. 8). The whole geological model was subjected to gravity loading in the vertical direction, which was automatically applied by the software. Based on previous studies (e.g., Zeng et al. 2010; Ju et al. 2018b; Xu et al. 2020), a compressive S_{Hmax} magnitude of approximately 165 MPa and a S_{hmin} magnitude of 140 MPa were laterally applied in the ~NNW-SSE

and ~ENE-WSW directions, respectively. Appropriate displacement constraints were applied to the geological model to prevent rotation and rigid displacement. In the numerical modeling results presented in Fig. 8, compressive and tensile stresses are indicated by negative and positive values, respectively.

Results and error analysis

The simulated results indicated that the S_{Hmax} magnitude ranged from - 150 to - 178 MPa, and the S_{hmin} magnitude varied between - 121 and - 157 MPa in the target Cretaceous layers of Bozi 3 Block (Fig. 9a, b). The S_{Hmax} and S_{hmin} showed similar distributions, where the negative values indicate that the Bozi 3 deep sandstone reservoir is subjected to compressive stresses. Gravity and boundary stresses play a major role in the study area. The stress values increased with the burial depth (Fig. 9).

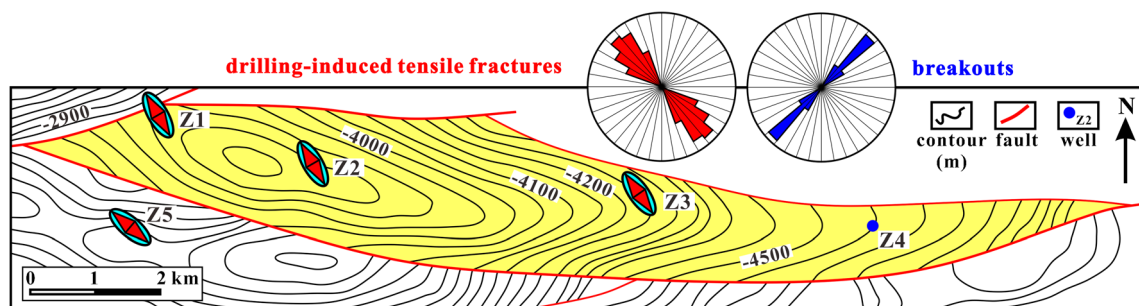


Fig. 5 The S_{Hmax} orientation interpreted from DITFs and breakouts in the Bozi 3 Block of Kuqa Depression

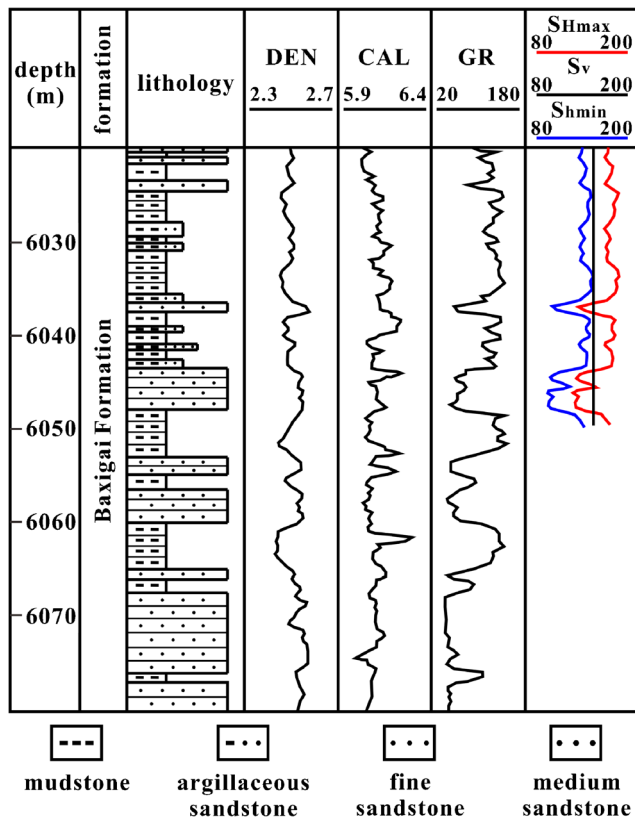


Fig. 6 Distribution of the present-day in situ stress magnitudes in Well Z1 of Bozi 3 Block based on well log calculations. Symbols: DEN, rock density, g/cm³; CAL, borehole diameter, cm; GR, gamma ray, API; units for stress magnitude are MPa

The Bozi 3 Block is currently in the exploration and initial development stage; hence, wide-spread fracturing and horizontal wells have not yet been deployed. Based on the above stress modeling results, an error analysis was carried out using Eq. (6): the errors between the measured and calculated stress

magnitudes were extremely low, generally less than 2% (Table 2), which suggests that the modeling results were credible.

$$r = \frac{|\text{calculated stress value} - \text{measured stress value}|}{\text{measured stress value}} \times 100\% \tag{6}$$

where *r* is the error between the calculated and measured value.

Implications for natural gas development

Effects of the stress field on natural fractures

In deep sandstone reservoirs, natural fractures favorably aligned with the present-day in situ stress field contribute considerably to subsurface fluid flows (Hillis 1997; Rajabi et al. 2016; Ju et al. 2020). Hence, the interpretations presented above show that fluid flows may be enhanced for natural fractures with strikes in the NNW-SSE direction. In addition, hydraulic fracturing is commonly required to increase gas production in deep sandstone reservoirs. During the hydraulic fracturing process, injecting fluids into target subsurface reservoir rocks may produce many geomechanically induced effects, such as the reactivation of natural fractures (Reynolds et al. 2003; Ju et al. 2020).

In this study, reactivation risk plots based on the Mohr's circle criterion (Mildren et al. 2002) are introduced to analyze the risk of natural fracture reactivation in the Bozi 3 deep sandstone reservoir. The location and pattern of the Mohr's circle in the shear stress-effective normal stress system is determined by the present-day in situ stress field calculated

Fig. 7 The geological model (a) and meshing results (b) of Bozi 3 Block of Kuqa Depression

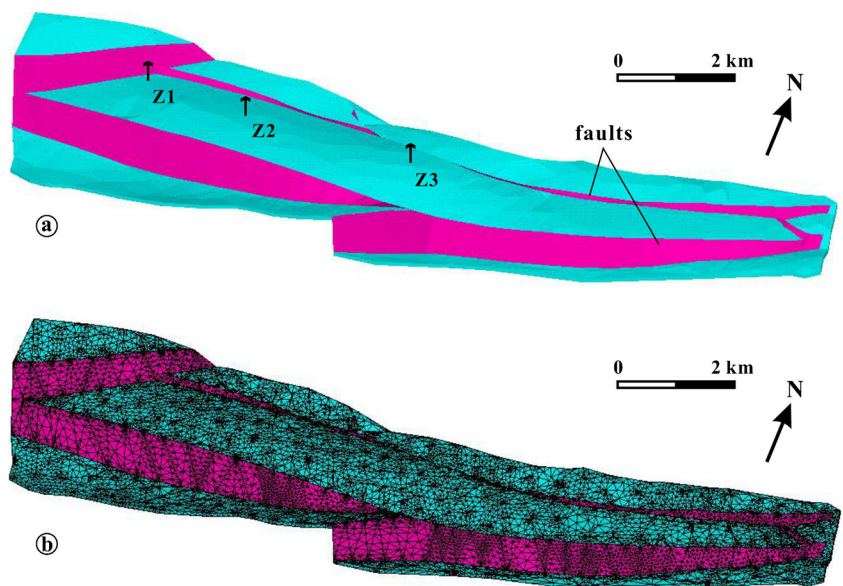


Table 1 Rock mechanics parameters used in this numerical study

Unit	Density ρ (kg/m ³)	Young's modulus E (GPa)	Poisson's ratio μ
Target layer	2500	36.0	0.25
Fault zone	2000	30.6	0.30
Nested model	2450	35.0	0.27

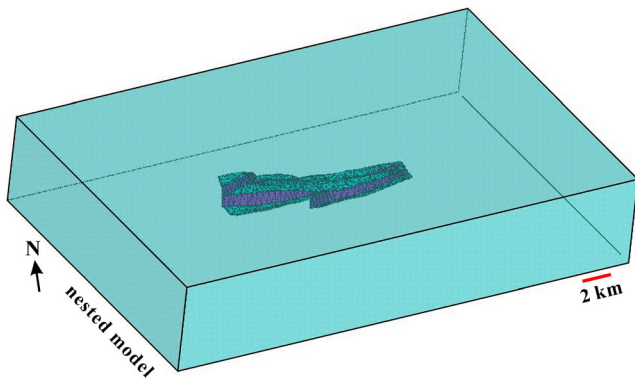
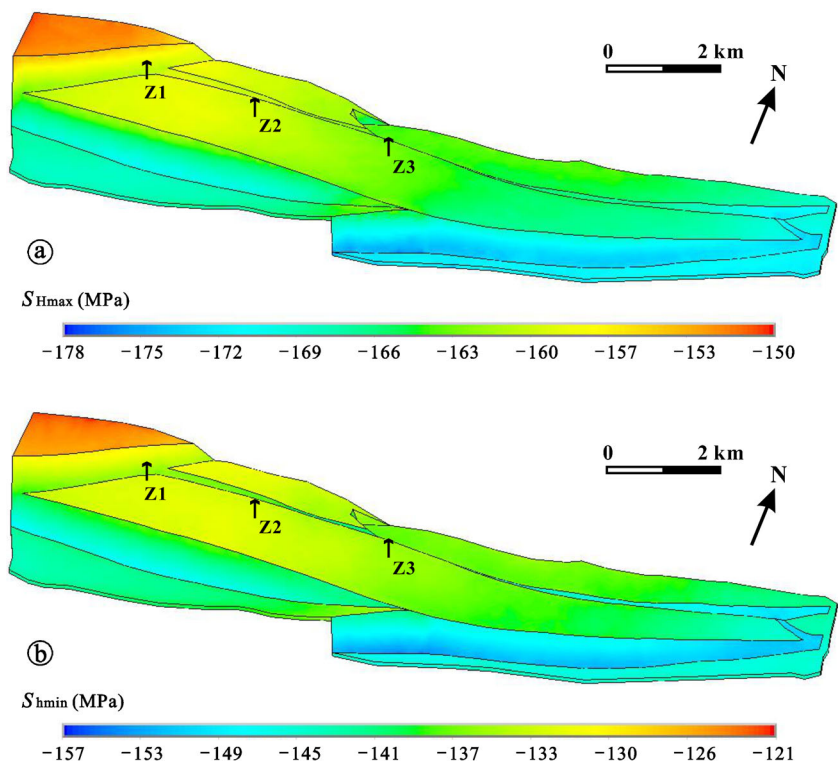


Fig. 8 The nested model used in this numerical analysis. The Bozi 3 Block is nested within a larger volume to reduce boundary effects and help apply forces

above. In the Mohr's Circle, dots (representing fractures) located on the right of the red critical line are stable and not reactivated (Fig. 10). In this study, Well Z3 and the natural fractures developed within this well are selected as examples for analysis. The plots are shown in Fig. 10 with warm colors (red) indicating the highest reactivation risk.

Fig. 9 The calculated S_{Hmax} (a) and S_{hmin} (b) magnitudes in the Bozi 3 Block of Kuqa Depression



The interpreted natural fractures with varying orientations clearly indicate different conditions under the present-day in situ stress state (Fig. 10). Natural fractures are generally stable in the present stress field. Injecting fluids into the reservoir rocks, shifting the Mohr's circle to the left, which increases the reactivation risk for natural fractures. In this study, when the specific gravity reaches 2.15, approximately 75% of all the interpreted natural fractures in Well Z3 are reactivated (Fig. 10), contributing to gas production.

Effects of stress state on hydraulic fractures

The present-day in situ stress field can influence hydraulic fracturing operations. Generally, a newly generated hydraulic fracture will propagate along the path that requires the minimum force (Kingdon et al. 2016). Hence, new horizontal wells should be drilled parallel to the S_{hmin} orientation. Based on the interpreted stress orientation (Fig. 5), horizontal wells in the Bozi 3 deep sandstone reservoir should be drilled following the ENE-WSW trend.

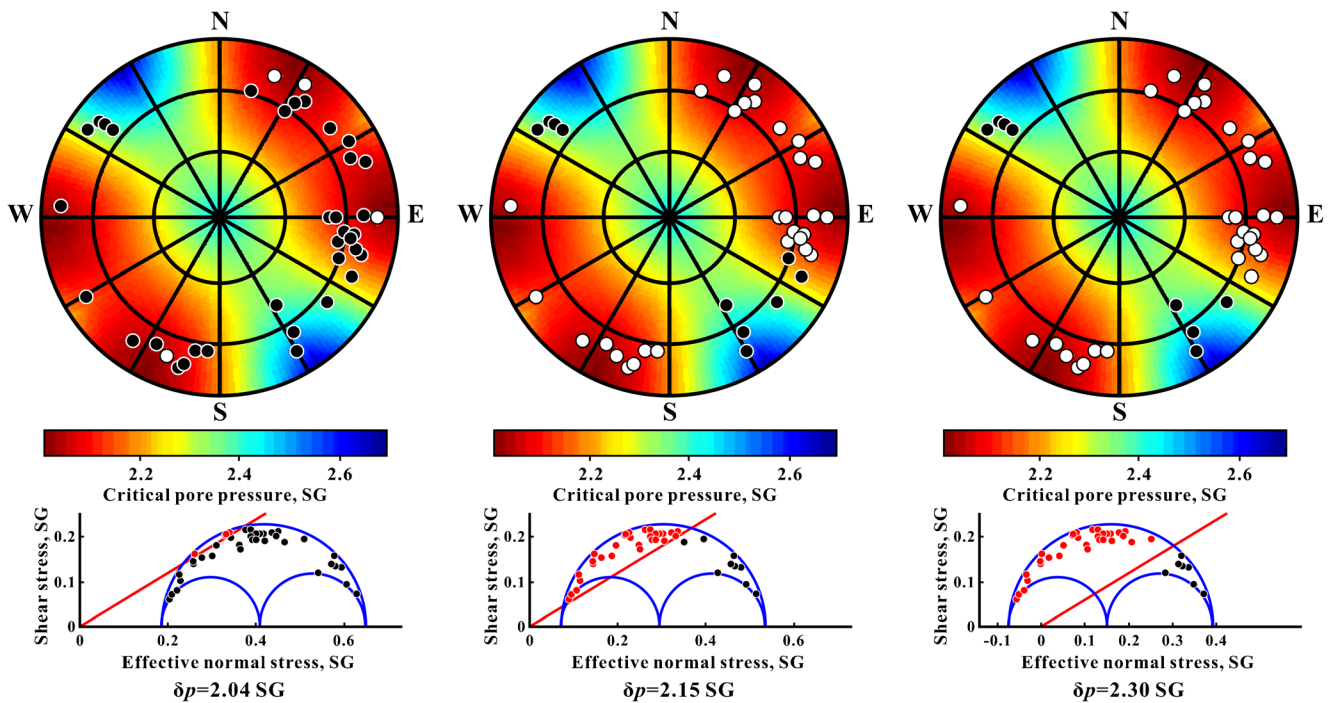


Fig. 10 Lower hemisphere stereonet plots and three dimensional Mohr circles showing critically stressed natural fractures in Well Z3 of Bozi 3 Block. The fracture orientations are plotted as the pole of planes with different colors representing the relative ease of fracture susceptibility as the amount of pore pressure increase required to reactivate a fracture. The red colors show the high likelihood of fracture reactivation, while the

blue colors indicate the low likelihood of reactivation for all possible fractures in the present-day stress state. Black and white dots in the stereonet plots are normal and critically stressed natural fractures, respectively. In the Mohr circles, black and red dots are normal and critically stressed natural fractures. SG is specific gravity, δp indicates the pore pressure increase

The parameter of the horizontal stress difference coefficient (K ; Eq. (7); Liu et al. 2020) is commonly used to determine the propagation of hydraulic fractures.

$$K = \frac{S_{Hmax} - S_{hmin}}{S_{hmin}} \tag{7}$$

Equation (7) can be used to obtain the spatial distribution of K in the study area. The main distribution of K can be described as follows: (1) the K values range from 0.14 to 1.53; and (2) the K values are controlled by depth, and are high in structurally high areas (Fig. 11). Generally, a small K facilitates the production of fracture networks (Liu et al. 2020). Based on the distribution pattern shown in Fig. 11, the areas around Well Z1 in the Bozi 3 Block are indicative of low K values, which may be viewed as engineering “sweet spots” for subsequent natural gas development.

Conclusions

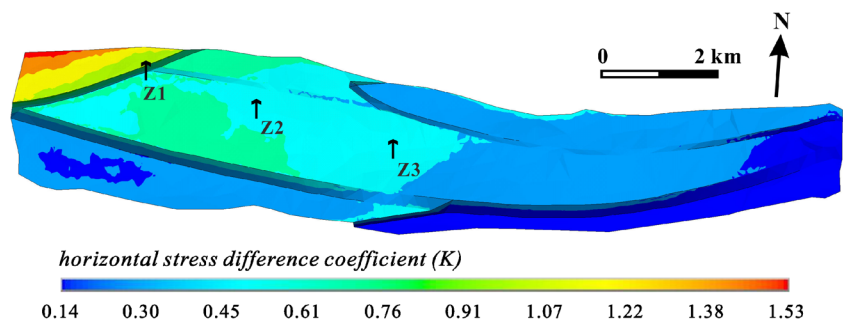
Knowledge of the present-day in situ stress field can facilitate deep gas exploration and development in the Bozi 3 Block of Kuqa Depression. In this study, the variation in stress magnitudes and stress orientations were analyzed based on well log calculations and numerical simulations, drilling-induced tensile fractures and borehole breakouts.

- (1) The S_{Hmax} orientation indicates a dominant NNW-SSE direction in the Bozi 3 Block, and it shows minor variations in different geological locations due to lithological differences and the development of faults and natural fractures.
- (2) Finite element stress simulation results show that the S_{Hmax} and S_{hmin} magnitudes in the Cretaceous layers of

Table 2 Error analysis of numerical stress results in the Bozi 3 Block

Well	Measured S_{Hmax} (MPa)	Calculated S_{Hmax} (GPa)	Error (%)	Measured S_{hmin} (MPa)	Calculated S_{hmin} (MPa)	Error (%)
Z1	161.54	160.96	0.35%	133.63	133.89	0.19%
Z2	159.76	162.10	1.46%	131.67	132.62	0.72%
Z3	166.67	164.56	1.27%	138.99	137.29	1.22%

Fig. 11 Distribution of the horizontal stress difference coefficient in the Bozi 3 Block of Kuqa Depression



Bozi 3 Block range between -150 and -178 MPa, and -121 and -157 MPa, respectively, indicating compression. Burial depth has considerable controlling effects on the stress magnitude distributions. Larger depths generally indicate higher stress magnitudes. The dominant stress regime indicates a strike-slip faulting type in the Cretaceous layers based on well log calculations.

- (3) Under the present-day in situ stress field in the Bozi 3 Block, horizontal wells should be drilled along the ENE-WSW trend. Nearly 75% of natural fractures are reactivated when the specific gravity reaches approximately 2.15. The areas around Well Z1 are the engineering “sweet spots” for gas development in the Bozi 3 Block.

Acknowledgements We would like to express our gratitude to the reviewers for their constructive suggestions and comments, which improved this manuscript in many aspects.

Funding This work was supported by the Natural Science Foundation of Jiangsu Province, China (BK20201349) and China Postdoctoral Science Foundation (2017T100419 and 2019M660269).

Declarations

Conflict of interest The authors declare that they have no competing interests.

References

- Allen MB, Vincent SJ (1999) Structural features of northern Tarim Basin: implications for region tectonics and petroleum traps: discussion. *Am Assoc Pet Geol Bull* 83:1279–1283
- Anderson EM (1951) The dynamics of faulting and dyke formation with applications to Britain, 2nd edn. Oliver, Edinburgh, p 206
- Bell JS (1996) Petro geoscience 2. In situ stresses in sedimentary rocks (part 2): Applications of stress measurements. *Geosci Can* 23(3): 135–153
- Brooke-Barnett S, Flottmann T, Paul PK, Busetti S, Hennings P, Reid R, Rosenbaum G (2015) Influence of basement structures on in situ stresses over the Surat Basin, southeast Queensland. *J Geophys Res Solid Earth* 120:4946–4965
- Ding WL, Fan TL, Yu BS, Huang XB, Liu C (2012) Ordovician carbonate reservoir fracture characteristics and fracture distribution forecasting in the Tazhong area of Tarim Basin, Northwest China. *J Pet Sci Eng* 86-87:62–70
- Dyman TS, Schmoker JW, Root DH (1998) USGS assesses deep undiscovered gas resource. *Oil Gas J* 96:99–103
- Feng JR, Gao ZY, Cui JG, Zhou CM (2016) The exploration status and research advances of deep and ultra-deep clastic reservoirs. *Adv Earth Science* 31(7):718–736 (in Chinese with English abstract)
- Fischer K, Henk A (2013) A workflow for building and calibrating 3-D geomechanical models—a case study for a gas reservoir in the North German Basin. *Solid Earth* 4:347–355
- Hillis RR (1997) Does the in situ stress field control the orientation of open natural fractures in sub-surface reservoirs? *Explor Geophys* 28(2):80–87
- Holditch SA (2006) Tight gas sands. *J Pet Technol* 58(6):86–93
- Jiu K, Ding WL, Huang WH, You SG, Zhang YQ, Zeng WT (2013) Simulation of paleotectonic stress field within Paleogene shale reservoirs and prediction of favorable zones for fracture development within the Zhanhua Depression, Bohai Bay Basin, east China. *J Pet Sci Eng* 110:119–131
- Ju W, Sun WF (2016) Tectonic fractures in the Lower Cretaceous Xiagou Formation of Qingxi Oilfield, Jiuxi Basin, NW China. Part two: numerical simulation of tectonic stress field and prediction of tectonic fractures. *J Pet Sci Eng* 146:626–636
- Ju W, Wang K (2018) A preliminary study of the present-day in-situ stress state in the Ahe tight gas reservoir, Dibeil Gasfield, Kuqa Depression. *Mar Pet Geol* 96:154–165
- Ju W, Shen J, Qin Y, Meng SZ, Wu CF, Shen YL, Yang ZB, Li GZ, Li C (2017) In-situ stress state in the Linxing region, eastern Ordos Basin, China: implications for unconventional gas exploration and production. *Mar Pet Geol* 86:66–78
- Ju W, Jiang B, Miao Q, Wang JL, Qu ZH, Li M (2018a) Variation of in situ stress regime in coal reservoirs, eastern Yunnan region, South China: implications for coalbed methane production. *Am Assoc Pet Geol Bull* 102(11):2283–2303
- Ju W, Li ZL, Sun WF, Xu HR (2018b) In-situ stress orientations in the Xiagou tight oil reservoir of Qingxi Oilfield, Jiuxi Basin, northwestern China. *Mar Pet Geol* 98:258–269
- Ju W, Niu XB, Feng SB, You Y, Xu K, Wang G, Xu HR (2020) Present-day in-situ stress field within the Yanchang Formation tight oil reservoir of Ordos Basin, central China. *J Pet Sci Eng* 187:106809
- Kingdon A, Fellgett MW, Williams JDO (2016) Use of borehole imaging to improve understanding of the in-situ stress orientation of Central and Northern England and its implications for unconventional hydrocarbon resources. *Mar Pet Geol* 73:1–20
- Liu JS, Yang HM, Wu XF, Liu Y (2020) The in situ stress field and microscale controlling factors in the Ordos Basin, central China. *Int J Rock Mech Min Sci* 135:104482

- Martin CD, Chandler NA (1993) Stress heterogeneity and geological structures. *Int J Rock Mech Min Sci Geomech Abstr* 30(7):993–999
- Mildren SD, Hillis RR, Kaldi J (2002) Calibrating predictions of fault seal reactivation in the Timor Sea. *APPEA Journal* 42:187–202
- Rajabi M, Tingay M, Heidbach O (2016) The present-day state of tectonic stress in the Darling Basin, Australia: Implications for exploration and production. *Mar Pet Geol* 77:776–790
- Reynolds S, Hillis R, Paraschivoiu E (2003) In situ stress field, fault reactivation and seal integrity in the Bight Basin, South Australia. *Explor Geophys* 34:174–181
- Tian J, Yang HJ, Wu C, Mo T, Zhu WH, Shi LL (2020) Discovery of Well Bozi 9 and ultra-deep natural gas exploration potential in the Kelasu tectonic zone of the Tarim Basin. *Nat Gas Ind* 40(1):11–19 (in Chinese with English abstract)
- Tingay M, Hillis RR, Morley CK, King RC, Swarbrick RE, Damit AR (2009) Present-day stress and neotectonics of Brunei: implications for petroleum exploration and production. *Am Assoc Pet Geol Bull* 93(1):75–100
- Wang YS (2012) Review of drilling fluid technique in deep wells with ultra-high temperature condition. *China High Technology Enterprises* 32:129–131 (in Chinese)
- Wei GQ, Wang JP, Zeng LB, Tang YL, Wang K, Liu TT, Yang Y (2020) Structural reworking effects and new exploration discoveries of subsalt ultra-deep reservoirs in the Kelasu tectonic zone. *Nat Gas Ind* 40(1):20–30 (in Chinese with English abstract)
- Xu K, Tian J, Yang HJ, Zhang H, Wang ZM, Yuan F, Wang HY (2020) Prediction of current in-situ stress field and its application of deeply buried tight sandstone reservoir: a case study of Keshen 10 gas reservoir in Kelasu structural belt, Tarim Basin. *J China Univ Min Technol* 49(4):708–720 (in Chinese with English abstract)
- Zeng LB, Wang HJ, Gong L, Liu BM (2010) Impacts of the tectonic stress field on natural gas migration and accumulation: a case study of the Kuqa Depression in the Tarim Basin, China. *Mar Pet Geol* 27:1616–1627
- Zeng QL, Mo T, Zhao JL, Tang YL, Zhang RH, Xia JF, Hu CL, Shi LL (2020) Characteristics, genetic mechanism and oil & gas exploration significance of high-quality sandstone reservoirs deeper than 7000 m: a case study of the Bashijiqi Formation of Lower Cretaceous in the Kuqa Depression. *Nat Gas Ind* 40(1):38–47 (in Chinese with English abstract)
- Zhang GY, Ma F, Liang YB, Zhao Z, Qin YQ, Liu XB, Zhang KB, Ke WL (2015) Domain and theory-technology progress of global deep oil and gas exploration. *Acta Pet Sin* 36(9):1156–1166 (in Chinese with English abstract)
- Zoback MD (2007) *Reservoir Geomechanics*. Stanford University, California, p 464
- Zoback MD, Barton CA, Brudy M, Castillo DA, Finkbeiner T, Grollmund BR, Moos DB, Peska P, Ward CD, Wiprut DJ (2003) Determination of stress orientation and magnitude in deep wells. *Int J Rock Mech Min Sci* 40:1049–1076